

# A SIMPLE MODEL FOR $r$ -PROCESS SCATTER AND HALO EVOLUTION

Brian D. Fields

*Center for Theoretical Astrophysics, Department of Astronomy, University of Illinois,  
Urbana, IL 61801, USA*

James W. Truran

*Department of Astronomy and Astrophysics and Enrico Fermi Institute, University of  
Chicago, Chicago, IL 60637, USA*

John J. Cowan

*Department of Physics and Astronomy, University of Oklahoma, Norman, OK 73019, USA*

## ABSTRACT

Recent observations of heavy elements produced by rapid neutron capture ( $r$ -process) in the halo have shown a striking and unexpected behavior: within a single star, the relative abundances of  $r$ -process elements heavier than Eu are the same as the same as those of solar system matter, while across stars with similar metallicity  $\text{Fe}/\text{H}$ , the  $r/\text{Fe}$  ratio varies over two orders of magnitude. In this paper we present a simple analytic model which describes a star's abundances in terms of its "ancestry," i.e., the number of nucleosynthesis events (e.g., supernova explosions) which contributed to the star's composition. This model leads to a very simple analytic expression for the abundance scatter versus  $\text{Fe}/\text{H}$ , which is in good agreement with the data and with more sophisticated numerical models. We investigate two classes of scenarios for  $r$ -process nucleosynthesis, one in which  $r$ -process synthesis events occur in only  $\sim 4\%$  of supernovae but iron synthesis is ubiquitous, and one in which iron nucleosynthesis occurs in only about 9% of supernovae. (the Wasserburg- Qian model). We find that the predictions in these scenarios are similar for  $[\text{Fe}/\text{H}] \gtrsim -2.5$ , but that these models can be readily distinguished observationally by measuring the dispersion in  $r/\text{Fe}$  at  $[\text{Fe}/\text{H}] \lesssim -3$ .

*Subject headings:* nuclear reactions, nucleosynthesis, abundances

## 1. Introduction

Neutron capture processes dominate the nucleosynthesis of elements beyond the iron peak. The physics of two neutron capture mechanisms has long been understood, and the astrophysical site for slow neutron capture nucleosynthesis (the *s*-process) has been shown to be low-mass stars (e.g., Busso, Gallino, & Wasserburg (1999)). However, the site for rapid neutron capture nucleosynthesis (the *r*-process) has not yet been unambiguously identified, although it is very likely connected to massive stars. The production site itself might be found in some or all Type II supernova (SN) events (e.g., Woosley, Wilson, Mathews, Hoffman, & Meyer (1994)), or in binary neutron star mergers (e.g., Eichler, Livio, Piran, & Schramm (1989); Rosswog, Davies, Thielemann, & Piran (2000)). Truran (1981) showed that the halo stars are a particularly useful laboratory for study of the *r*-process, as the observed neutron capture abundance patterns in these stars indicate that the *s*-process component drops out, and the *r*-process dominates, as one looks at stars with  $[\text{Fe}/\text{H}] \lesssim -2.2$  (Burris et al. (2000)). Recent years have shown that halo stars indeed give unique insight into the *r*-process. With the advent of high dispersion, high S/N measurements, the abundance observations within and among halo stars has led to surprising new discoveries with important consequences for theories of the *r*-process as well as halo formation.

The halo star with perhaps the most striking *r*-process composition is CS 22982-052. With  $[\text{Fe}/\text{H}] = -3.1$ , this is an ultra-metal-poor star;<sup>1</sup> its abundance ratios through the iron peak are typical for a halo star. However, this star also has been observed in 20 *r*-process elements from barium upwards (the “heavy” *r*-process), with abundances (Sneden et al. (1996; 2000))

$$\left[ \frac{r}{\text{Fe}} \right] \simeq 1.7 \quad \Rightarrow \quad \frac{r}{\text{Fe}} \simeq 50 \left( \frac{r}{\text{Fe}} \right)_{\odot} \quad (1)$$

The element-to-element scatter in this ratio is consistent with the observational errors. This remarkable trend does *not* appear to hold for the “light” *r*-process,  $40 < Z < 56$  (Sneden et al. (2000)). Nevertheless, the fact that the heavy *r*-process elements agree so well with each other is stunning, given that this star could well have abundances that reflect the nucleosynthesis of a single supernova, while the solar abundances average over many generations of supernovae. The strong implication is that there is a *unique* astrophysical site for the *r*-process (at least for the heavy *r*-elements, which for brevity we will refer to simply as “*r*-elements” hereafter).

This result has profound implications. First, the mere presence of *r*-process in very metal-poor stars points to origins associated with massive stars. Moreover, given the appar-

---

<sup>1</sup>In the standard notation,  $[A/B] = \log(A/B)_{\star} - \log(A/B)_{\odot}$ ; we take ultra-metal-poor stars to be those with  $[\text{Fe}/\text{H}] < -2.5$ .

ent *universality* of the  $r$ -process, one might expect that all ratios among  $r$ -process nuclides to always be constant (with pollution by the  $s$ -process increasing with  $[\text{Fe}/\text{H}]$ ). This leads to the prediction that at the lowest metallicities, when the  $s$ -process has not turned on, ratios among  $r$ -process elements should be fixed and the same across all stars. So far this appears to be true in the other ultra-metal-poor star for which there is similarly good data, HD 115444 (Westin, Sneden, Gustafsson, & Cowan (2000)), which has  $[\text{Fe}/\text{H}] = -3.0$  and  $[r/\text{Fe}] = 0.96$ . Very recently, Cayrel et al. (2001) have shown that CS 31082-001 (with  $[\text{Fe}/\text{H}] = -2.91$ ) has Os/Fe and Ir/Fe abundances which give  $[r/\text{Fe}] = 1.98$  and  $R = 96$ . This would be the highest  $r$ -process overabundance yet observed. Clearly, a systematic study of  $r$ -process abundance patterns in this star is of the highest priority (particularly since this is the first star in which uranium has been detected).

CS 22892-052 and HD 115444 have iron abundances that are identical within errors, and both show a remarkable constancy in their  $r/\text{Fe}$  ratios for different  $r$ -elements *within each star*. However, these stars show a significant *difference* in their mean  $r/\text{Fe}$  ratios. This is an example of the large scatter in  $r/\text{Fe}$  ratios that has been observed in halo stars. As we will see, the dispersion in  $r/\text{Fe}$  ratios is small at  $[\text{Fe}/\text{H}] \gtrsim -1$ , but grows with decreasing metallicity, finally spanning two orders of magnitude for ultra-metal-poor stars. The observed large scatter in  $r/\text{Fe}$  in Pop II stars — and the very high  $r/\text{Fe}$  in a few — demands that *not all stars make both the  $r$ -process and iron*.

Models for  $r$ -process nucleosynthesis and for Pop II chemical evolution must account at once for the remarkable constancy of  $r/\text{Fe}$  among different elements within individual stars, as well as for the variability of  $r/\text{Fe}$  between stars. These facts together suggest the following simple picture for Pop II  $r/\text{Fe}$ . We assume that the observed Pop II  $r/\text{Fe}$  abundances in each star reflect  $r$ -process contributions of a *few* supernovae. The basic idea is that

- Different  $r/\text{Fe}$  arise from different mixing between the dominant  $r$ -process sources and the dominant Fe sources; and
- The  $r/\text{Fe}$  scatter then reflects the amount of mixing between the two sources.

The key is the inhomogeneity of the halo, which this scheme in fact quantifies.

This scenario makes quantitative predictions:

1. There is a maximum to  $r/\text{Fe}$ , which is the  $r/\text{Fe}$  production ratio in those stars which produce  $r$ -process elements, undiluted by any ( $r$ -poor) Fe events
2. The minimum to  $r/\text{Fe}$  is the  $r/\text{Fe}$  ratio in the  $r$ -poor events. This minimum may be as small as  $r/\text{Fe} = 0$ .

3. The placement of a star between these extremes quantifies a admixture of nucleosynthesis sources recorded in the star. Thus, (a) at the very earliest times, when single SN events are really all that contaminate a given star, the  $r/\text{Fe}$  scatter should *only* populate the extremes. (b) At later times, but before mixing is efficient, the regions between the extremes will be filled in. (c) At still later times, mixing becomes efficient, and then the scatter decreases towards a "universal" mix of the two sources.

If this line of reasoning is correct, it has the very significant implication that  $r/\text{Fe}$  becomes a *tracer* of the inhomogeneity of the halo. One can see the transition from single to multiple events, and also the transition from multiple sources to a well mixed Galaxy. The details of these transitions allow one to correlate metallicity and mixing. And we can at least grossly confirm the time sequence of the nucleosynthesis events.

Several groups have used similar arguments to motivate detailed models which explain  $r/\text{Fe}$  scatter in terms of  $r$ -process nucleosynthesis and an inhomogeneous chemical evolution of the Galactic halo. Ishimaru & Wanajo (1999) construct a one-zone model for the halo, but introduce abundance dispersion through a Monte Carlo realization of individual supernova events with yields of Fe and Eu which are strong function of mass. They obtain good fits to the observed scatter for models in which the  $r$ -process is produced by a small fraction of supernovae. Argast, Samland, Gerhard, & Thielemann (2000) use similar  $r$ -process progenitor masses, but drop the assumption of one-zone evolution. They model the spatial inhomogeneity and incomplete mixing of expanding supernova remnants in the halo, and again find good agreement with the observed Eu/Fe dispersion.

The goal of the present paper is to aid in the understanding of these detailed models, and to help focus attention on the key physics relevant for this problem. We will show (§2) that the  $r/\text{Fe}$  scatter follows quite generally from the stochastic behavior of the halo chemical evolution, and that one can derive simple, explicit, analytical expressions for the abundance scatter as a function of metallicity. We will do this for two scenarios, one in which the  $r$ -process occurs in only a small fraction of supernovae but Fe is ubiquitous (§2.1), and the scenario of Wasserburg & Qian (2000), in which the converse holds (§2.2). Fortunately, these scenarios can be distinguished by future measurements of  $r/\text{Fe}$  scatter in ultra-metal-poor stars, and we present observational strategies to do this (§3). Discussion and conclusions appear in §4.

## 2. Two Scenarios for $r$ -process Origin

The  $r/\text{Fe}$  scatter demands that the  $r$ -process and iron are not co-produced in the same ratios in the same events, but rather there will be  $r$ -rich and  $r$ -poor events. Also, very high and very low  $r/\text{Fe}$  ratios are observed. The highest  $r/\text{Fe}$  event observed places a lower limit on the  $r/\text{Fe}$  yields of the  $r$ -rich events. Furthermore, the fact that the highest  $r/\text{Fe}$  is much larger than the Pop II mean implies that the  $r$ -rich, high  $r/\text{Fe}$  events occur at a very different rate than low  $r/\text{Fe}$  events. One can envision either “iron-dominated” schemes in which high  $r/\text{Fe}$  events are rare, but iron-producing events are not; or, alternatively, the possibility that  $r$ -process events are the more common, with iron-producing events rarer. We now consider each of these scenarios in turn.

### 2.1. Iron-dominated Models

We assume (1) that the supernova  $r$ -process yields are *bimodal*, i.e., that some supernovae have a high  $r$ -process yield and others a low one (possibly zero); and (2) for simplicity, we assume not only that all supernovae make iron, but also that the Fe yield takes the same constant value for all supernovae.<sup>2</sup> With these assumptions, supernova ejecta can take one of two values of  $r/\text{Fe}$ . We will denote the objects with the larger  $r/\text{Fe}$  ratio as class  $A$ , and those with the lower ratio as class  $B$ . We purposely avoid a more descriptive nomenclature—e.g., “high” and “low”—as we wish to avoid both confusion (high yields? rates? masses?) and prejudice with regard to the nature of the progenitors which are the dominant  $r$  producers. To simplify notation, we will define the scaled  $r/\text{Fe}$  ratio to be

$$R \equiv \frac{r/\text{Fe}}{(r/\text{Fe})_{\odot}} \quad (2)$$

which implies that  $[r/\text{Fe}] = \log R$ .

Thus, a supernova will produce a fixed amount of iron, and yields  $r$ -elements at either the high value  $R_a$  or the low value  $R_b$ . Denote the fraction of class  $A$  supernovae (averaged over the halo IMF) to be  $f_a$ ; then the fraction of class  $B$  supernovae is of course  $f_b = 1 - f_a$ .

The  $r/\text{Fe}$  data show that at a metallicity  $\text{Fe}/\text{H} \sim -1$ ,  $[r/\text{Fe}]$  converges to a value of  $\sim 0.3$ , i.e.,  $\bar{R} \sim 2$ .<sup>3</sup> We take this value as the mean  $R$  attained when averaging over a large

---

<sup>2</sup>It is possible that some supernovae make neither  $r$  nor Fe; if such events exist, they are irrelevant to the present discussion.

<sup>3</sup>Above this metallicity  $r/\text{Fe}$  decreases, but this is presumably due to the addition of the Fe yields of

sample of progenitors, whose fractions reflect the underlying  $f_a$  and  $f_b$  dictated by the IMF. Thus we have that

$$\bar{R} = f_a R_a + f_b R_b = R_b + f_a (R_a - R_b) \quad (3)$$

We can use the observed scatter to estimate the values of  $R_a$  and  $R_b$ . The highest observed is  $[r/\text{Fe}] \simeq 1.7$  (eq. 1); we take this as a measure of  $R_a \simeq 50$ . On the other hand, the lower limit of the  $r/\text{Fe}$  scatter is not as well determined. The available data suggests that the minimum, if any, differs depending on the elemental  $r$ -tracer used. At most, we have  $[r/\text{Fe}]_{\min} \sim -0.6$ , giving  $R_b \simeq 0.25$ ; it is also possible that  $[r/\text{Fe}]_{\min} \sim -1.7$ , giving  $R_b = 0.02 \simeq 0$ . Upper limits to  $r/\text{Fe}$  have not been reported, but this may be a selection effect. A key issue is whether there *could have been* lower  $r/\text{Fe}$  values than the ones reported; such information places useful constraints on  $r$ -process production. For our purposes, as long as  $R_b \ll \bar{R}$ , then we may take  $R_b = 0$ , as we will now see.

Once one establishes the observed values for  $\bar{R}$ ,  $R_a$ , and  $R_b$ , then the relative numbers of class *A* and *B* supernovae is now *fixed*. Eq. (3) gives

$$f_a = \frac{\bar{R} - R_b}{R_a - R_b} \simeq \frac{\bar{R}}{R_a} \quad (4)$$

where the last expression uses the observed fact that  $R_b/\bar{R} \ll 1$ . For  $\bar{R} = 2$  and  $R_a = 50$ , eq. (4) gives  $f_a = 3.5\%$  for  $R_b = 0.25$ , and  $f_a = 4.0\%$  for  $R_b = 0$ . Thus we see that observed fact of the very large  $r/\text{Fe}$  variations immediately implies that class *A* events are *required* to be uncommon, regardless of their physical nature. That is, *the events which produce the r-process originate from a small fraction,  $\sim 4\%$ , of all massive stars.*

### 2.1.1. Basic Model

Using these numbers, we are now in the position to model the scatter of  $r/\text{Fe}$ . To do this, we create a set of halo stars and deduce the history—the nucleosynthetic ancestry—of each. We assume that each of the halo stars we create incorporates gas which has been enriched by some number  $N_{\text{SN}}$  of supernova of either type: this is the number of supernova ancestors for the star. We create stars by allow  $N_{\text{SN}}$  to run from 1 to  $N_{\text{max}}$ , and sample equal intervals in  $N_{\text{SN}}$ . Note that we are free to chose the number of halo stars we create, and that this number is unrelated to the number of supernova ancestors assigned to a given halo star.

---

Type Ia supernovae. We do not include these events (and implicitly assume their  $r$ -process yield to be zero); thus we will not attempt to model  $r/\text{Fe}$  at  $[\text{Fe}/\text{H}] > -1$ .

The metallicity follows from the assumption that all stars have the same iron yield, so that  $\text{Fe}/\text{H} \propto N_{\text{SN}}$ . We introduce a parameter  $(\text{Fe}/\text{H})_{\text{min}}$ , the iron enrichment from a single star. Then  $\text{Fe}/\text{H} = N_{\text{SN}}(\text{Fe}/\text{H})_{\text{min}}$ , and  $[\text{Fe}/\text{H}] = [\text{Fe}/\text{H}]_{\text{min}} + \log N_{\text{SN}}$ .

The  $r$ -process pattern of the stars is also fixed in terms of the stellar ancestry. We assume that the mean value of  $R$  for our population of stars is always  $\bar{R}$ .<sup>4</sup> We then introduce scatter around  $\bar{R}$  by sampling stars whose ancestry (in class  $A$  and  $B$  stars) is a random variable. The underlying physics of this random process is ultimately controlled by the physics of  $r$ -process nucleosynthesis and the mixing of stellar ejecta. However, even in the absence of this detailed physics, simple assumptions allow for a stochastic behavior that resembles the observations. We will illustrate two such simple assumptions regarding the random distribution of “ancestors.”

First, we treat  $N_a$ , the numbers of ancestors of class  $A$ , as a *discrete* random variable. That is, we imagine that the number ancestors from each class take integer values. We choose  $N_a$  from a binomial distribution with mean  $\bar{N}_a = f_a N_{\text{SN}}$ ; it then follows that  $N_b = N_{\text{SN}} - N_a$ . For each star, the fraction of class  $A$  (high  $r$ ) progenitors is  $f_{a,*} = N_a/N_{\text{SN}}$ , and

$$R_* = f_{a,*} R_a + f_{b,*} R_b = R_b + (R_a - R_b) N_a/N_{\text{SN}} \quad (5)$$

The dispersion in  $N_a$  naturally induces a dispersion in  $R_*$ :  $\sigma(R_*) = (R_a - R_b) \sigma(N_a)/N_{\text{SN}}$ . Since  $\sigma(N_a) \sim \sqrt{N_a}$ , this gives

$$\sigma(R_*) \simeq (R_a - R_b) \sqrt{N_a}/N_{\text{SN}} \simeq \bar{R}/\sqrt{N_a} = (f_a \text{Fe}/\text{Fe}_{\text{min}})^{-1/2} \bar{R} \quad (6)$$

where we have assumed successively that  $f_b \simeq 1$  and  $R_b \ll \bar{R}$ . Thus we see that the fractional error in  $R$  is just given by the counting statistics of  $N_a$ :  $\sigma(R_*)/\bar{R}_* \simeq 1/\sqrt{N_a}$ . We now can put each star on the  $(r/\text{Fe}, [\text{Fe}/\text{H}])$  plane, and the model is complete.

This model thus has three free parameters which can be fixed by observations:  $\bar{R}$ ,  $R_a$ , and  $R_b$ ; there is one parameter,  $(\text{Fe}/\text{H})_{\text{min}}$  which is (for now) determined by theory. We can rewrite eq. (6) explicitly in terms of these parameters:

$$\sigma_R = (f_a \text{Fe}/\text{Fe}_{\text{min}})^{-1/2} \bar{R} \quad (7)$$

and thus

$$\sigma_{[r/\text{Fe}]} = \frac{1}{f_a^{1/2} \ln 10} 10^{-([\text{Fe}/\text{H}] - [\text{Fe}/\text{H}]_{\text{min}})/2} = 10^{-([\text{Fe}/\text{H}] + 3.3)/2} \quad (8)$$

---

<sup>4</sup>As long as both classes  $A$  and  $B$  exist; below we will consider the effect when there is a time delay before the onset of one class. The constancy of  $r/\text{Fe}$  can be determined observationally. Current data samples the low metallicities too sparsely to make a strong statement (Burris et al. (2000)), but with more observations one should be able to test for a metallicity dependence of  $r/\text{Fe}$ .

The model thus predicts that the intrinsic scatter in  $r/\text{Fe}$  falls as  $(\text{Fe}/\text{H})^{-1/2}$ . As we will see, this is indeed consistent with the halo star data. Of course, the data also contain observational errors, both in  $[r/\text{Fe}]$  and  $[\text{Fe}/\text{H}]$ . We include these in the model, using  $\sigma([r/\text{Fe}])_{\text{obs}} = 0.10$  dex, and  $\sigma([\text{Fe}/\text{H}])_{\text{obs}} = 0.05$  dex, with the supposition that the errors are uncorrelated with the intrinsic dispersion.

Results for a Monte Carlo realization of a population drawn from a binomial distribution appear in Figure 1. The predicted envelope is shown, and provides a reasonable fit for the observed data. Note that the envelope includes both the observational errors as well as the intrinsic scatter given by (eq. 7). In the binomial model just described, there are quantization effects due to the integral values of  $N_i$ . These are particularly noticeable when  $\bar{N}_a < 1$ , which occurs when  $N_{\text{SN}} < 1/f_a \simeq 25$ , or  $[\text{Fe}/\text{H}] \lesssim -2.6$ . In this regime, most points will cluster at  $R_b$ , with only a few at higher values. Furthermore,  $R = \bar{R}N_a/N_{\text{SN}}$  is also quantized. The lower envelope of the nonzero values is given by the case when  $N_a = 1$ , so that  $R_{\text{env}} = \bar{R}/N_{\text{SN}}$  and  $[r/\text{Fe}]_{\text{env}} = -\text{Fe}/\text{H} + \log \bar{R}$ ; this is clearly seen in Figure 1.

One need not require that a star’s heavy element ancestry be quantized in this way. For example, one can plausibly imagine that the mixing of successive generations of supernova ejecta is not an “all or nothing” prospect, but rather that a given parcel of ISM gas and dust can be enriched to different degrees by the ancestors it had. This is indeed very likely to be the case, which would mean that the quantization effects of the binomial model are spurious (and thus the binomial results are only to be trusted in the regime where  $\bar{N}_a > 1$ , or  $[\text{Fe}/\text{H}] \gtrsim -2.6$ ).

Thus, it is of interest to consider making the number of ancestors of each class a continuous random variable. This can be done in a way that naturally generalizes from the binomial distribution; in that case, the total number of supernova progenitors  $N_{\text{SN}}$  is fixed, and the *fraction*  $f = N_a/N_{\text{SN}}$  of progenitors of class  $A$  is a random variable which has a mean  $\langle f \rangle = f_a$  but can take only discrete rational values due to the integral nature of  $N - a$ . We will continue to take  $N_{\text{SN}}$  to be fixed, but we will now assume that the fraction  $f$  of progenitors of class  $A$  is now a continuous random variable, with mean  $\langle f \rangle = f_a$ . We thus want to draw  $f$  from a continuous distribution with values in the interval  $[0, 1]$  and with a fixed mean. These requirements are met by the beta distribution, which has a distribution function

$$\xi(x) = \frac{1}{\text{B}(a, b)} x^{a-1} (1-x)^{b-1} \quad (9)$$

for  $f \in [0, 1]$  and where  $\text{B}(a, b)$  is the beta function, which can be expressed in terms of the gamma function  $\text{B}(a, b) = \Gamma(a)\Gamma(b)/\Gamma(a+b)$ . We fix the parameters  $a$  and  $b$  of the distribution by simultaneously fitting the mean  $\langle f \rangle = a/(a+b)$  to the observed value  $f_a$ , and forcing the variance  $\sigma^2(f) = ab(a+b)^{-2}(a+b+1)^{-1}$  to the same value as the



binomial case,  $\sigma^2(f) = f_a(1 - f_a)/N_{\text{SN}}$ . These conditions are satisfied if  $a = f_a(N_{\text{SN}} - 1)$  and  $b = (1 - f_a)(N_{\text{SN}} - 1)$ .

Our procedure is to draw  $f$  according to the beta distribution  $\xi(f)$ . We then find  $N_a = fN_{\text{SN}}$  and  $N_b = (1 - f)N_{\text{SN}} = N_{\text{SN}} - N_a$ . Since  $f$  is a continuous variable, so are  $N_a$  and  $N_b$ . Our choices of the parameters  $a$  and  $b$  guarantee that  $\langle R \rangle = \bar{R}$  and that  $\sigma(R)$  is identical to the value found for the binomial case, so that eqs. (6) and (7) still hold. Results for a Monte Carlo simulation of a stellar population appear in Figure 2. We see that the general trend is quite similar to that for the binomial case, but that the continuous nature of the parent distribution guarantees that quantization effects are now absent. We see that at the very lowest metallicities  $[\text{Fe}/\text{H}] \lesssim -3.5$ , the points cluster at  $r/\text{Fe}_{\text{min}}$ , and have a mean value below that at higher metallicity. This feature has a similar origin to that of its counterpart in Figure 1. At the lowest metallicities, the small number statistics in the SN parents is a dominant effect, and the  $r$ -rich events are too rare to be expected in a sample of the size presented here.

A comparison with the observed data in Figure 2 shows that the beta distribution model gives a good fit to the available data. We thus conclude that the observed scatter in  $r/\text{Fe}$  may be understood by our simple scenario in which halo stars stochastically sample the yields of two different populations of heavy element producing events. In this interpretation, the degree of scatter increases with decreasing metallicity due to counting statistics, so that the lowest-metallicity events record the nucleosynthesis of a few ( $N_{\text{SN}} = \text{Fe}/\text{Fe}_{\text{min}}$ ) events. Furthermore, since  $\sigma(R)/\bar{R} \simeq \sqrt{f_a}/N_{\text{SN}}$ , a good measure of the scatter in  $r/\text{Fe}$  allows one to find  $N_{\text{SN}}$  and thus one can fix the parameter  $(\text{Fe}/\text{H})_{\text{min}}$ . In this way, one can empirically measure the single-event iron yield, and also determine the number of nucleosynthesis events recorded at a particular metallicity. The fact that the observed distribution is reasonably enclosed by the theory curves which use  $[\text{Fe}/\text{H}]_{\text{min}} = -4$  (e.g., Audouze & Silk (1996)) indicates that this value is a reasonable first approximation.

### 2.1.2. *Introducing Stellar Lifetimes*

Having achieved a reasonable fit to the data, we are emboldened to consider refinements to this model. Specifically, we turn to the question of timescales. Thus far, we have implicitly assumed that there is always the same relative probability of  $r$ -rich and  $r$ -poor nucleosynthesis events. However, this assumption is likely to break down at very early times. One expects that the two classes  $A$  and  $B$  of nucleosynthesis events stem from different physics. For example, the  $r$ -rich and  $r$ -poor classes could correspond to progenitor stars with different masses and thus different lifetimes, or  $r$ -process production could arise from binary neutron

star mergers, and thus require some time delay for inspiral. In either case, one expects a time lag between the first events of one class versus the first events of the other. During this initial period, the  $r/\text{Fe}$  ratio of the ISM and of any new stars will be only that of the allowed class of nucleosynthesis events. There will thus be no dispersion in  $r/\text{Fe}$  or rather, the dispersion will be due to the smaller intrinsic dispersion within the allowed class. Once events of the other class can occur,  $r/\text{Fe}$  dispersion will set in, and the  $r/\text{Fe}$  will scatter around its mean value.

We can crudely simulate this time delay between the onset of the two classes as follows. We note that the iron abundance increases with time. Thus, a time delay can be encoded as a delay in  $\text{Fe}/\text{H}$ . We choose a value  $(\text{Fe}/\text{H})_{\text{cut}}$  as the cutoff that marks the onset of the lagged class of nucleosynthesis events. To allow for dispersion in the birth times of the first stars, we introduce some randomness in this cutoff by making the cutoff number  $N_{\text{cut}}$  of events a poisson random variable, with mean  $\bar{N}_{\text{cut}} = \text{Fe}_{\text{cut}}/\text{Fe}_{\text{min}}$ . We then require that if  $N_{\text{SN}} < N_{\text{cut}}$ , only events of the allowed class  $i$  can occur, and thus  $R = R_i$ . If  $N_{\text{SN}} > N_{\text{cut}}$ , then we follow the standard procedure described above.

Results appear in Figure 3, using  $\text{Fe}_{\text{cut}} = 10 \text{ Fe}_{\text{min}}$ , which roughly corresponds to timescales  $\tau_{\text{long}} = 10 \tau_{\text{short}}$ , where the longer lifetime is that of the species cut off. As expected, we see that the very low  $\text{Fe}/\text{H}$ , the dispersion vanishes and the points lie at the level of the allowed class. While this is clearly an oversimplified description, it nevertheless gives a qualitative sense of the kind of behavior one expects if there is indeed a significant disparity between the timescales for the production of  $r$ -rich and -poor events. A discrepancy in timescales is required if the  $r$ -process production “switch” is related the progenitor star’s mass. As we suspect the mass to be the controlling parameter, our prediction is that one of the panels in Figure 3 represents the trend that will be observed in ultra-metal-poor stars.

Thus, a discovery of the sort of behavior seen in Figure 3 would indicate which class has the sorter production timescale, and thus provide a key clue as to the astrophysical origin of the dominant  $r$ -process site. Furthermore, a determination of  $\text{Fe}_{\text{cut}}/\text{Fe}_{\text{min}}$  would help to quantify (in a model-dependent way) the time delay itself. If class  $A$  stars have the longer timescale,  $\tau_a > \tau_b$ , then physically this means that (1) the  $r$ -process producers evolve more slowly and thus (2) these stars should show up later, so that there should be a limiting low metallicity below which all stars have  $R_{\star} = R_b$ . The appearance of the first stars with  $R_{\star} > R_b$  marks the time of the first  $r$ -process stars and thus  $t \geq \tau_a$ .

We can be more specific by using the fact that  $r$ -process stars must be a small fraction of all supernovae. This means that the progenitors must represent a limited range in the massive star IMF: either  $8 - 10M_{\odot}$  or  $\gtrsim 25M_{\odot}$ . If  $\tau_a$  is long, this would select the  $8 - 10M_{\odot}$  range, and thus mean that  $\tau_a \simeq \tau(10M_{\odot}) \simeq 3 \times 10^7$  yr. Now consider the opposite case. If

$A$  stars have the shorter timescale, the  $\tau_a < \tau_b$ , and the  $r$ -process stars should appear first. Consequently, there should be a limiting low metallicity below which all stars have  $R_\star = R_a$ , and the appearance of the first stars with  $R_\star < R_a$  marks the time of the first non- $r$ -process stars and thus  $t \geq \tau_b$ . The short  $\tau_a$  implies the high mass ( $m \gtrsim 25M_\odot$ ) progenitor mass range, and thus  $\tau_b \gtrsim \tau(25M_\odot) \simeq 10^7$  yr.

While massive stars seem required to explain the  $r$ -process simply due to their evolutionary timescale, it is possible that the  $r$ -process is not made in the core collapse and explosion, but rather through the merger of supernova remnants, via neutron star-neutron star mergers (e.g., Eichler, Livio, Piran, & Schramm (1989); Rosswog, Davies, Thielemann, & Piran (2000)). As pointed out recently by Qian (2000), an important constraint on this scenario comes from magnitude of the halo star  $r/\text{Fe}$  scatter, which appears to be too small (!) to reconcile with the low merger rate and thus high yields of the coalescence events. An additional issue for neutron star coalescence is the timescale of the merger, which is an extra delay in the appearance of the  $r$ -process compared to the other supernova products (such as iron). This timescale is a strong function of the orbital semimajor axis and particularly eccentricity (Peters (1964)). As shown in population synthesis calculations (e.g., Fryer, Woosley, & Hartmann (1999)), this leads to a wide distribution of inspiral timescales, spanning a few Myr to  $\sim 1$  Gyr. Thus, if the  $r$ -process does come from binary neutron star mergers, then the first events had to have the correct orbital parameters to allow a very rapid evolution.

Finally, even if observations establish the *lack* of a signature of the kind seen in Figure 3 would provide useful information about the  $r$ -process as well. We would learn that there is no significant difference in the timescales for production of the two classes of events. This would rule out any models which require such a delay, and would challenge the presumption that the  $r$ -process yields are a function of the mass of the progenitor stars. Alternatively, it may suggest a very different scenario entirely, as we now shall see.

## 2.2. $r$ -process-dominated Models

In the previous section, we assumed that  $r$ -process nucleosynthesis events are rare, while iron production events are ubiquitous (for massive stars). We now turn to the reverse case, which has been developed in some detail by Wasserburg & Qian ((2000); hereafter, WQ2000). The essential ingredients are the following, in chronological order: (1) “Pop III.” A very rapid burst of star formation produces an uneven Galactic floor of  $[\text{Fe}/\text{H}] \sim -4$  to  $-3$ , but no  $r$ -process. The inhomogeneity of this population will lead to  $r/\text{Fe}$  scatter in this metallicity range. (2) “Pure  $r$ -process.” The first of the Pop II supernovae produce the (heavy)  $r$ -process

without any Fe. These are WQ2000’s high-frequency  $H$  events. (3) “Fe added.” After  $\sim 10$   $H$  lifetimes, the first iron-producing supernovae go off. These make the light  $r$ -process (i.e., sub-barium, which we do not consider here), but *none* of the heavy  $r$ -process. They occur at lower frequency and thus are dubbed  $L$  events.

We model the Wasserburg & Qian scenario as follows; our approach and some details are very similar to the model discussed in the previous section. WQ2000 note that the Pop III events need not occur in a homogeneous or well-mixed way, which will lead to global  $[\text{Fe}/\text{H}]$  variations between  $-4$  and about  $-3$ . Thus, we assume that a single Pop III parent would have ejecta which mix with its surroundings, leading to an enrichment of  $[\text{Fe}/\text{H}] = [\text{Fe}/\text{H}]_{\text{min,III}} = -4$ ; this is the Pop III iron yield. This sets the Fe floor. These events do not make any  $r$ -process, which raises the possibility of an observable abundance record of this stage remains, as we will discuss shortly. It is possible, indeed it is likely, that the first stars of the next stage of Galactic evolution form prior to the onset of first  $H$  events which make the first  $r$ -process elements. Any such stars will have only Pop III abundances and thus will be void of any  $r$ -process. The number of such  $r$ -free stars depends on the details of star formation immediately after Pop III, and thus are difficult to estimate. We will thus make the simple assumption that the first  $H$  events are not significantly delayed after the formation of the first halo stars, so that there is not a significant population of Pop III,  $r$ -free stars.

In the next stage, the Pop II stars commence. The pure- $r$   $H$  events occur first, as they have lifetimes 10 times shorter than those of the Fe-only  $L$  events. Each  $H$  event is taken to produce the same  $r$ -process yield, and thus the total  $r$ -production is just the number  $N_h$  of parents times the yield of a single event. Once the  $L$  events commence, they produce only Fe (and the light  $r$ -process, which we don’t consider). WQ2000 put the Fe yield of a single event to be about  $[\text{Fe}/\text{H}]_\ell = -2.5$ , i.e., 30 times more than that of the Pop III events. We assume all  $L$  events have this yield.

We thus have two epochs to model. The first is the period after the Pop III events but before the first  $L$  event, and the second is the rest of the Pop II phase, up to  $[\text{Fe}/\text{H}] = -1$ . We begin modeling each halo star’s ancestry by determining which of these epochs it samples. To do this, we choose a metallicity in the range  $-4 \leq [\text{Fe}/\text{H}] \leq -1$ .<sup>5</sup> We note that whenever  $[\text{Fe}/\text{H}] < [\text{Fe}/\text{H}]_\ell = -2.5$ , then the star must have arisen in the first,  $H$ -only epoch, and have no  $L$  event progenitors. In this case, the number of Pop III progenitors is then fixed to be

---

<sup>5</sup>Again, we are free to sample any metallicity in this range, as we are not modeling the massive stars but only the present-day halo stars which record the nucleosynthetic past.

$$N_{\text{III}} = \text{Fe}/\text{Fe}_{\text{min,III}}.^6$$

We then determine the number of  $H$  events in our halo star’s lineage, by choosing  $N_h$ . As in the previous section, we note that the specific distribution of  $N_h$  is determined by the detailed physics of star formation and gas dynamics in the earliest epoch in our Galaxy. The distribution is constrained by the  $H$  event-to- $L$  event ratio of 10, which demands that on average, there are 10  $H$  events before the first  $L$  event occurs. Independent of the specific distribution, a crucial issue is the expected correlation between  $N_h$  and  $N_{\text{III}}$  (and thus Fe). Since these events occur in two different phases by two different population, we will make the simple assumption that the two are uncorrelated. We then have  $R_\star = r_h N_h / \text{Fe}$ , with Fe already fixed and with  $r_h$  the  $r$ -process yield of a single  $H$  event (determined below). Note that since  $N_h$  is uncorrelated with Fe, then the mean trend  $\langle R \rangle = \langle N_h \rangle r_h / \text{Fe}$  which scales as  $\text{Fe}^{-1}$ . That is, the mean  $r/\text{Fe}$  trend for  $-4 \leq [\text{Fe}/\text{H}] \leq -2.5$  should not be constant, but should decrease with logarithmic slope -1. Scatter about the  $r/\text{Fe}$  trend is created by the variance in  $N_h$ :  $\sigma_R = \sigma(N_h) r_h / \text{Fe} = \sigma(N_h) / N_h R$ . For illustration, we will choose  $N_h$  from a uniform distribution. in  $(0, 10)$ , which gives  $\langle R \rangle = 5 r_h / \text{Fe}$ , and  $\sigma_R / R = 1/\sqrt{3}$ .

We now turn to the case of stars for which we have picked a higher  $\text{Fe}/\text{H} > \text{Fe}/\text{H}_\ell$ . For these stars, some contribution by iron-producing  $L$  events is necessary. As before we generate a number  $N_{\text{SN}}$  of supernova parents for each halo star. Thus, each star generated has  $N_h$   $H$  parents and  $N_\ell$   $L$  parents, but the star’s iron abundance constrains our choice of  $N_\ell$  and thus  $N_{\text{SN}}$ . Namely, the star has a metallicity

$$(\text{Fe}/\text{H})_\star = N_{\text{III}}(\text{Fe}/\text{H})_{\text{min,III}} + N_\ell(\text{Fe}/\text{H})_\ell = (N_{\text{III,eff}} + N_\ell) (\text{Fe}/\text{H})_\ell \quad (10)$$

with  $N_{\text{III,eff}} = (\text{Fe}_{\text{min,III}}/\text{Fe}_\ell) N_{\text{III}}$ . We choose  $N_{\text{III}}$  from a distribution between 0 and  $\text{Fe}_\ell/\text{Fe}_{\text{min,III}} \simeq 30$ ; for illustration, we will use the uniform distribution. Once given  $N_{\text{III}}$ , then  $N_\ell$  is fixed by eq. (10).

Turning to  $N_h$ , we must choose this in a way that is consistent with our choice of  $N_\ell$ . Note that since the  $L$  events are 10 times rarer, the variance in  $N_\ell$  is much larger than that in  $N_h$ , and thus we should expect a large span in the allowed  $N_h$  choice at fixed  $N_\ell$ . We proceed by first estimating the total number of supernova events to be  $\hat{N}_{\text{SN}} = N_\ell / f_\ell$ , where  $f_\ell = 1/11 = 1 - f_h$  is the fraction of supernova of type  $L$ . Using a beta distribution, we choose  $f_{\ell,\star}$ , with  $a = f_\ell(\hat{N}_{\text{SN}} - 1)$  and  $b = f_\ell(\hat{N}_{\text{SN}} - 1)$ . We then have  $f_{h,\star} = 1 - f_{\ell,\star}$ , and can determine  $N_{\text{SN},\star} = N_\ell / f_{\ell,\star}$ . From these, we find  $N_h = f_{h,\star} N_{\text{SN},\star} = f_{h,\star} / f_\ell N_\ell$ , and the

---

<sup>6</sup>This may not be an integer, but we will interpret fractional progenitor numbers as indicative of partial mixing, as done in the previous section.

star’s  $r/\text{Fe}$  ratio,

$$R_{\star} = \frac{N_h}{N_{\text{III,eff}} + N_{\ell}} R_{\text{yld}} \quad (11)$$

where  $R_{\text{yld}} = r_h/\text{Fe}_{\ell}$  is the ratio of the (number) yields from the two event types. Note that at high metallicity, we have  $N_h, N_{\ell} \gg N_{\text{III,eff}}$  and thus

$$R_{\star} \longrightarrow \frac{N_h}{N_{\ell}} R_{\text{yld}} \longrightarrow \bar{R} \quad (12)$$

But since Wasserburg & Qian specify that H events occur 10 times more frequently than L events, we have  $N_h/N_{\ell} = 10$ , and from eq. (12) we can infer the proper  $R_{\text{yld}} = r_h/\text{Fe}_{\ell}$  parameter to give the correct  $\bar{R}$ . Namely, we have  $R_{\text{yld}} = \bar{R}/10 = 0.2$ , and  $r_h = \text{Fe}_{\ell} R_{\text{yld}} = 6.3 \times 10^{-4}$ .

We now turn to the  $r/\text{Fe}$  dispersion at  $\text{Fe}/\text{H} > \text{Fe}/\text{H}_{\ell}$ . Note that simple analytic formulae are not easily derived for the  $r/\text{Fe}$  scatter in the WQ2000 scenario, owing to the presence of random variables in both the numerator and denominator of eq. (11). Nevertheless, one can roughly estimate that  $\sigma(R)/R \sim 1/\sqrt{N_{\ell}}$ . For  $\text{Fe} > \text{Fe}_{\ell}$ , this gives an intrinsic dispersion of  $\sigma(R)/R \sim \sqrt{\text{Fe}/\text{Fe}_{\ell}}$ , the same  $\text{Fe}^{1/2}$  scaling as that in the Fe-dominated case.

Results from a Monte Carlo realization appear in Figure 4. the dashed curve shows the  $2\sigma$  envelope which includes observational errors and the intrinsic scatter predicted by  $\sigma(R)/R = \sqrt{\text{Fe}/\text{Fe}_{\ell}}$  and plotted over its range of validity. We see that the scatter at  $[\text{Fe}/\text{H}] > -2.5$  is similar to that in the Fe-dominated case, and in reasonable agreement with the present data. However, the low metallicity convergence behavior seen in Figure 3 does not appear in the Wasserburg & Qian scenario. Rather, at  $[\text{Fe}/\text{H}] < -2.5$  we see the  $R \sim 1/\text{Fe}$  trend discussed above. We again conclude that observations of the  $r/\text{Fe}$  scatter in this regime can thus provide important information about  $r$ -process astrophysics.

### 3. Observational Tests of $r$ -Process Astrophysics

The models we have presented for  $r/\text{Fe}$  scatter all show similar trends from  $\text{Fe}/\text{H} = -1$  down to about  $-2.5$ . However, below this metallicity, the differences become increasingly stark, as seen in the figures. The predicted behaviors are for points to cluster above, below, or around the mean value  $[r/\text{Fe}]_{\text{avg}}$ .

- If the points all cluster around  $[r/\text{Fe}] \gg [r/\text{Fe}]_{\text{avg}}$ , this points to a very early population which, regardless of the small number of ancestors, maintained high  $r/\text{Fe}$ . This would confirm that the earliest stars produced both iron and  $r$ -elements, and thus that the sources of the  $r$ -process are short-lived and thus high-mass stars.

- If, conversely, the points all cluster around  $[r/\text{Fe}] \ll [r/\text{Fe}]_{\text{avg}}$  (or which have only upper limits for  $r$ -process elements), this indicates that the earliest stars produced iron but failed to produce significant  $r$ . This is thus evidence for a delay until the first  $r$ -producing stars, and thus points to longer-lived progenitors (lower mass supernovae or NS-NS binaries).
- Finally, the points could continue to cluster around  $[r/\text{Fe}]_{\text{avg}}$ . This would indicate that the earliest stars could collectively produce *both* the  $r$ -process or iron, but the persistent scatter would demand that *individual* stars could only produce one of the two. This points to a picture of the kind suggested by Wasserburg & Qian, wherein an early (and non-uniform) Pop III production of iron is quickly followed by rapid production of iron-free  $r$ -process ejecta.

Thus we see that ultra-metal-poor stars can provide “smoking gun” evidence for  $r$ -process astrophysics.

#### 4. Conclusions

We have presented an analytical approach to understanding the scatter in  $r$ -process-to-iron ratios in metal-poor halo stars. The observed  $r/\text{Fe}$  scatter demands that the bulk of the  $r$ -process and of iron cannot be produced in the same stars. We have used a simple stochastic description of the different populations of nucleosynthesis events which contribute to  $r$ -process and iron abundances in each halo star. The random star-to-star variations in nucleosynthetic “ancestry” lead to scatter in  $r/\text{Fe}$ . The models we present are all successful in reproducing the scatter in the available data, which go down to about  $[\text{Fe}/\text{H}] = -3$ . We see that the abundance scatter can be understood simply in terms of the variance due to counting statistics of the ancestry of each star. We present simple and convenient analytic expressions for the scatter in this regime.

We model two basic scenarios for  $r$ -process production; one in which the  $r$ -process is rare, occurring in about  $\sim 4\%$  of all massive stars. The other scenario, that of WQ2000, takes the reverse approach in which  $r$ -process production is ubiquitous and iron production rare in massive stars.<sup>7</sup> We find that these scenarios give very similar  $r/\text{Fe}$  scatter at  $[\text{Fe}/\text{H}] \gtrsim -2.5$ , but show divergent behavior at lower metallicity. Observations in this regime can discriminate among these scenarios and give important clues regarding the lifetimes and

---

<sup>7</sup>In the final stages of completion of this paper, we became aware of the work of Qian (2001), which also considers  $r/\text{Fe}$  scatter in the WQ2000 model. His methods and conclusions are very similar to ours.

thus the masses of the astrophysical  $r$ -process production sites. We therefore strongly urge an observational effort to measure  $r$ -process abundances (and upper limits!) in the ultra-metal-poor halo stars.

We thank Roberto Gallino, John Lattanzio, Chris Sneden, and Ron Webbink for useful discussions. This research has received support from NSF grant AST-9986974 to J.J.C. and from DOE contract B341495 to J.W.T.

## REFERENCES

- Argast, D., Samland, M., Gerhard, O.E., & Thielemann, F.-K. 2000, *A&A*, 356, 873
- Audouze, J., & Silk, J. 1996, *ApJ*, 451, L49
- Burris, D.L., et al. 2000, *ApJ*, 544, 302
- Busso, M., Gallino, R., & Wasserburg, G.I. 1999, *ARAA*, 37, 239
- Cayrel, R., et al. 2001, *Nature*, 409, 691
- Edvarsson, B., et al. 1993, *A&A*, 275, 101
- Eichler, D., Livio, M., Piran, T., & Schramm, D. N. 1989, *Nature*, 340, 126
- Fryer, C.L., Woosley, S.E., & Hartmann, D.H. 1999, *ApJ*, 526, 152
- Ishimaru, Y., & Wanajo, S. 1999, *ApJ*, 511, L33
- Jehin, E., et al. 1999, *A&A*, 341, 241
- Kalogera, V., & Lorimer, 1997, *ApJ*, 489, 244
- McWilliam, A. 1998, *AJ*, 115, 1640
- McWilliam, A., Preston, G.W., Sneden, C. & Searle, L. 1995a, *AJ*, 109, 2757
- McWilliam, A., Preston, G.W., Sneden, C., & Schectman, S. 1995b, *AJ*, 109, 2736
- Peters, P.C. 1964, *Phys. Rev.*, 136, B1224
- Qian, Y.-Z. 2000, *ApJ*, 534, L67
- Qian, Y.-Z. 2001, *ApJL*, submitted



- Sneden, C., et al. 1996, ApJ, 467, 819
- Sneden, C., et al. 2000, ApJ, 533, L139
- Rosswog, S., Davies, M. B., Thielemann, F. -K. & Piran, T. 2000, A&A, 360, 171
- Truran, J.W. 1981, A&A, 97, 391
- Wasserburg, G.J., & Qian, Y.Z. 2000, ApJ, 529, L21 (WQ2000)
- Westin, J., Sneden, C., Gustafsson, B., & Cowan, J.J. 2000, ApJ, 530, 783
- Woolf, V.M., Tomkin, J. & Lambert, D.L. 1995, ApJ, 453, 660
- Woosley, S.E., Wilson, J.R., Mathews, G.J., Hoffman, R.D., & Meyer, B.S. 1994, ApJ, 433, 229

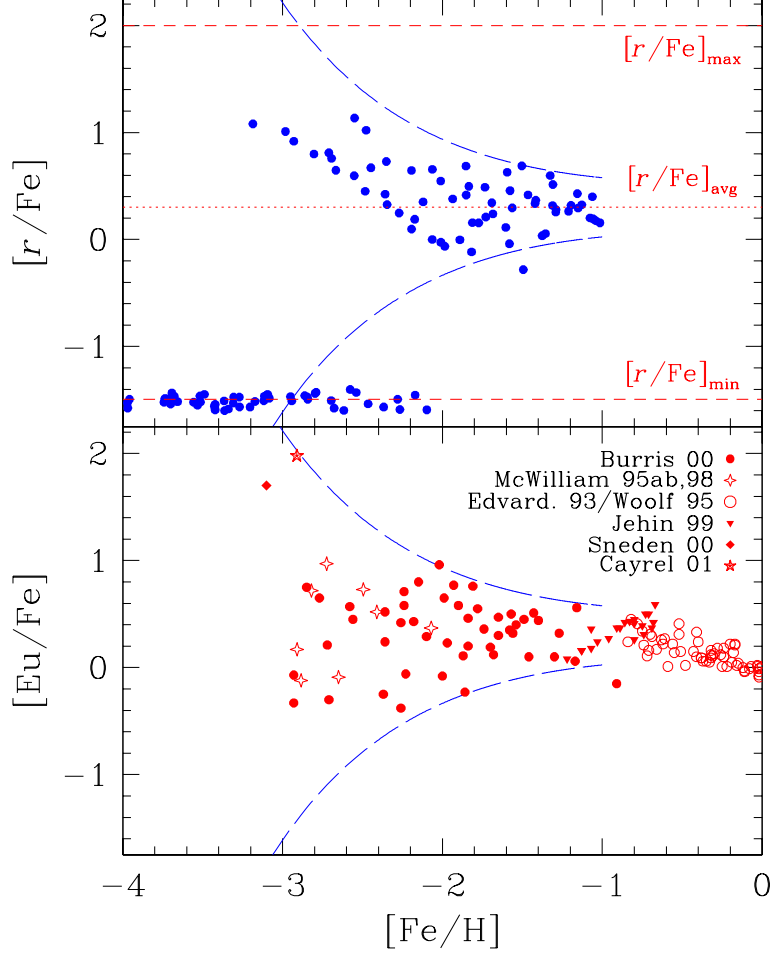


Fig. 1.— Distribution of  $r/\text{Fe}$  abundances for halo stars. *Upper panel:* model calculation. The points represent stars whose ancestry has been drawn according to a binomial distribution. In addition to the intrinsic dispersion calculated in the model, we have included random observational errors with zero mean and standard deviation  $\sigma_{[R]} = 0.15$  and  $\sigma_{[\text{Fe}/\text{H}]} = 0.10$ . *Lower panel:* observed data for  $[\text{Eu}/\text{Fe}]$ ; references are as shown. For CS 31082-001 (Cayrel et al. (2001)) Eu abundances are as yet unavailable, so the average of  $[\text{Os}/\text{Fe}]$  and  $[\text{Ir}/\text{Fe}]$  is used. The dashed curves in both panels are the analytic relation for the  $2 - \sigma$  envelope predicted from this model (eq. 7). The curves are drawn to account for the logarithmic nature of the plot, ie., the curves are located at the  $2\sigma$  limits, namely  $\log \bar{R} \pm 2 \log 10\sigma(R)/\bar{R}$ .

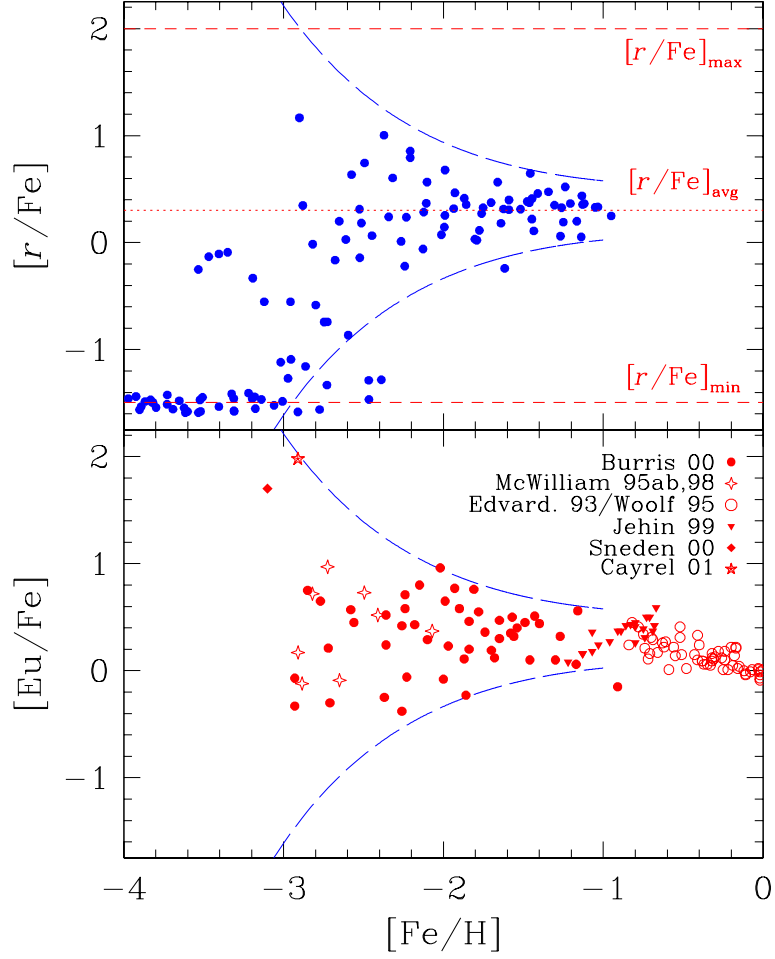


Fig. 2.— As in Figure 1, for the beta distribution model. Due to the continuous nature of the parent distribution, the quantization effects seen in the binomial case are now absent.

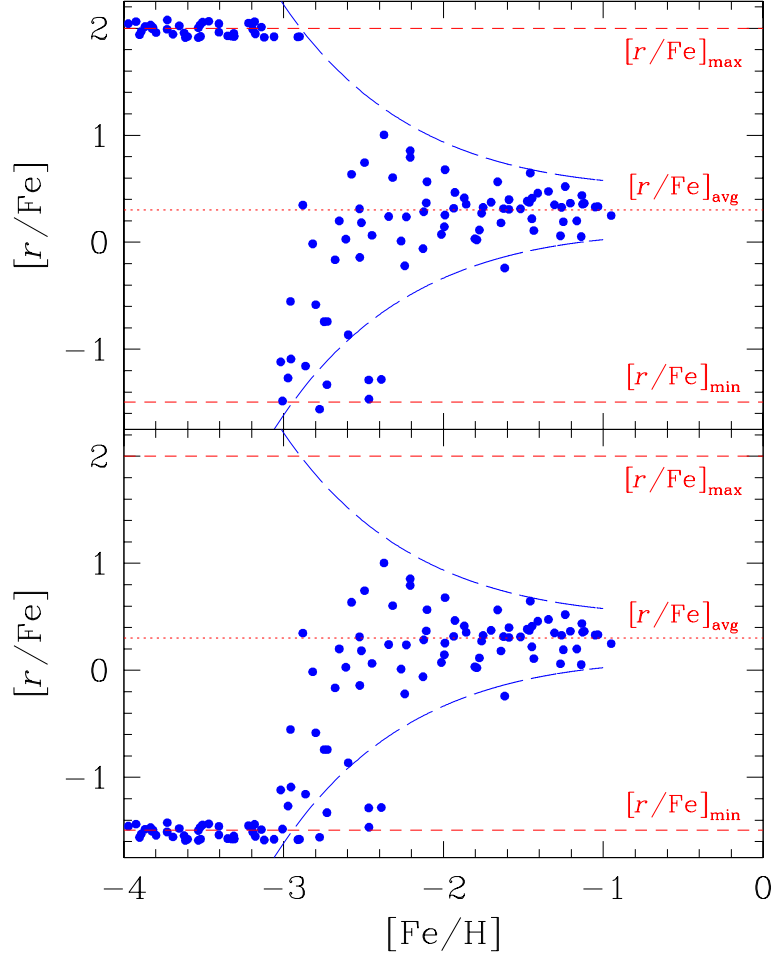


Fig. 3.— Predicted  $r/\text{Fe}$  distributions, with timescale information encoded through metallicity cutoffs. *Upper panel:* a delay has been imposed on class  $B$  ( $r$ -poor) events, so that class  $A$  events dominate at early times. *Lower panel:* a delay has been imposed on class  $A$  events.

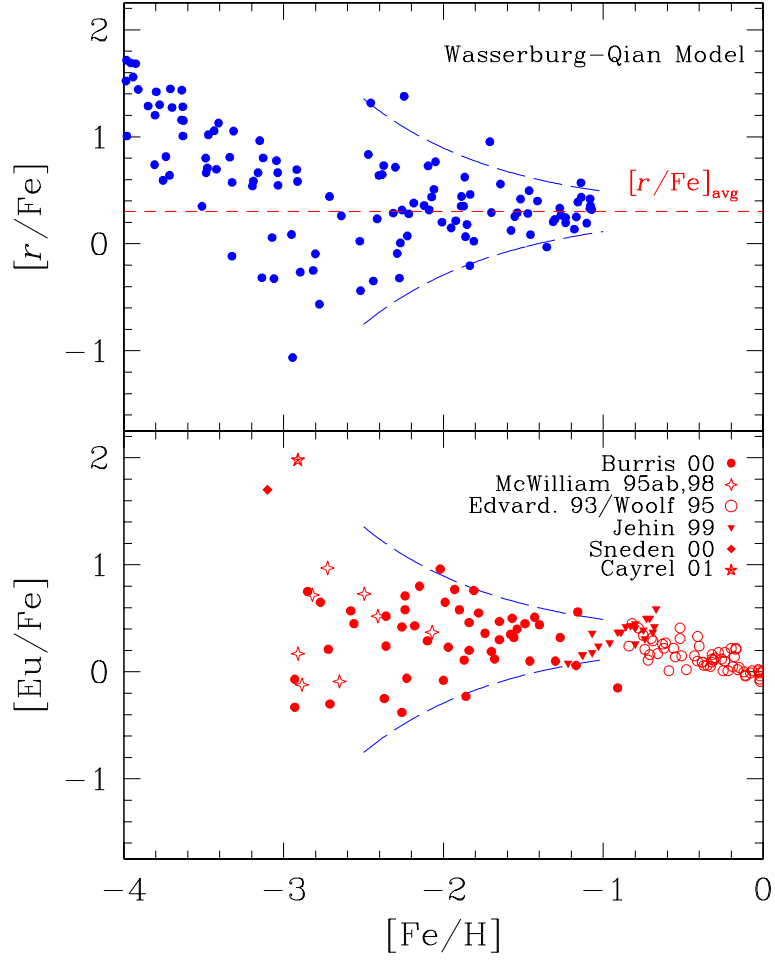


Fig. 4.— As in Figure 1, for the Wasserburg & Qian (2000) model.